Borneo Journal of Pharmacy
Vol 8 Issue 4 November 2025
Pages 353 – 367

https://journal.umpr.ac.id/index.php/bjop/article/view/7435
DOI: https://doi.org/10.33084/bjop.v8i4.7435
e-ISSN: 2621-4814

Research Article

Kelor (*Moringa oleifera*) Bioactive Compounds as Potential Anti-Breast Cancer Agents: *In Silico* Studies

Saeful Amin *

Vanessa Angelica Sheryl

Ade Yeni Aprillia

Anisa Pebiansyah

Department of Pharmacy, Universitas Bakti Tunas Husada, Tasikmalaya, West Java, Indonesia

*email: saefulamin@universitas-bth.ac.id; phone: +6285223746389

Keywords:
Breast anticancer
Computational studies
Estrogen
Moringa Leaves

Abstract

Breast cancer is the most common type of cancer in women. Kelor (*Moringa oleifera*) leaves are a plant with medicinal properties for treatment. This study aimed to determine the activity and identify the metabolite compounds of *M. oleifera* leaves that are more effective and stable at the estrogen receptor (ER), potentially serving as an anticancer agent for breast cancer. The methods employed are computational studies, including molecular docking, PKCSM tests, and molecular dynamics simulations. The results of a computational molecular docking study of 23 *M. oleifera* leaf compounds identified the three best compounds from the docking results of the best ER genistein compounds on the 1QKM receptor, as well as genistein and luteolin compounds on the 1X7J receptor, all with low free energy values. From the pkCSM test of 23 compounds, three compounds were selected that showed good absorbance and distribution, and the toxicity prediction indicated that one compound did not exhibit hepatotoxicity. Molecular dynamics results for the Luteolin 1X7J compound, simulated for 100 ns, showed lower and more stable RMSD and RMSF values compared to those of compounds on the ER.

Received: June 24th, 2024
1st Revised: August 5th, 2025
2nd Revised: October 19th, 2025
Accepted: November 6th, 2025
Published: November 30th, 2025

INTRODUCTION

Breast cancer, medically known as *carcinoma mammae*, is a prevalent malignancy that affects both women and men, arising from the mammary glands, fatty tissue, or connective tissue of the breast. It ranks among the most common malignant tumors globally; for instance, studies indicate that breast cancer is the most frequently diagnosed malignant tumor in Chinese women, with its incidence steadily increasing annually. Early diagnosis and effective treatment are therefore crucial for reducing associated mortality rates[1,2].

Current standard treatments for breast cancer typically involve chemotherapy, hormone therapy, and surgery. However, the efficacy of these conventional therapies remains limited, particularly for patients with advanced-stage disease. Consequently, recent research has focused on developing targeted therapeutic pathways, often involving the identification of specific molecular receptors to inhibit cancer progression[3,4].

One crucial molecular target is the Estrogen receptor-alpha (ER-α). Estrogen stimulates gene expression and cell proliferation, and ER-α plays a pivotal role in the development and progression of breast cancer. As a ligand-inducible transcription factor, ER-α can be leveraged to regulate the growth, survival, and differentiation of breast cancer cells, making it a highly relevant target for drug development[5,6].

In the pursuit of new therapeutic agents, natural products have become increasingly important resources for drug discovery[7]. Moringa or Kelor (*Moringa oleifera* L.) is a plant widely used as both food and traditional medicine globally,

How to cite: Amin S, Sheryl VA, Aprillia AY, Pebiansyah A. Kelor (Moringa oleifera) Bioactive Compounds as Potential Anti-Breast Cancer Agents: In Silico Studies. Borneo J Pharm. 2025;8(4):353-67. doi:10.33084/bjop.v8i4.7435

valued for its established antioxidant, anti-inflammatory, and anticancer properties. The plant contains over 100 secondary metabolites, including key compounds such as quercetin, kaempferol, genistein, eugenol, and luteolin[8-10]. Previous research has confirmed the diverse biological activities of *M. oleifera*, spanning antibacterial, antitumor, and general anticancer effects[11].

To rapidly screen and predict the efficacy of these natural compounds, molecular docking is employed as an essential *in silico* method in rational drug design[12,13]. This computational technique predicts the molecular interaction and affinity between a small molecule (ligand) and the active site of a target protein (receptor). By analyzing the three-dimensional structure of the resulting complex, docking identifies potential therapeutic candidates and predicts their activity at the molecular level. This study aims to utilize the molecular docking to determine the anticancer activity of compounds present in *M. oleifera* leaves, specifically by predicting their binding and inhibitory potential against relevant breast cancer receptors.

MATERIALS AND METHODS

Materials

This study utilized a combination of hardware, standalone software, and web-based computational platforms. The hardware specifications included an Intel® Core™ i7-3632QM CPU (2.2 GHz, Turbo Boost 3.2 GHz), 4.00 GB of RAM, and a 64-bit Operating System. The primary software packages employed were MarvinSketch (for compound drawing/preparation), YASARA and PLANTS (for docking procedures), and Discovery Studio (for visualization and analysis). Web-based resources included the PubChem database for ligand information, the Protein Data Bank (PDB) for receptor files, pkCSM for ADME/Tox prediction, Google Colabs for data processing, and a tool for assessing the Lipinski Rule of Five (Ro5). The study focused on 23 compounds selected based on previous literature identifying them as active constituents of *M. oleifera* leaves. These were compared against established breast cancer drugs: cyclophosphamide, docetaxel, and paclitaxel. The target receptors were ERs, specifically obtained from the PDB website (https://www.rscb.org/) under the PDB codes 2QA8, 1X7R, 1X7J, 1QKM, and 6QGG (all in PDB file format), which represent anti-breast cancer targets.

Methods

Receptor and ligand preparation

The study utilized multiple estrogen-related receptor (ERR) structures, specifically those with PDB IDs 2QAB, 1X7R, 1X7J, 1QKM, and 6QGG, which were downloaded in .pdb format from the PDB website. The stereochemical quality of each receptor was rigorously assessed using the Ramachandran plot analysis via the PDBSum web server. Receptor preparation, including the removal of native ligands, was conducted using YASARA software. For ligand preparation, 2D structures of the test compounds were downloaded from the PubChem database. These structures were then imported into MarvinSketch for geometry optimization, which included protonation to determine the major microspecies. The optimized structures were saved in .mrv format. Conformational analysis was then performed by generating conformers and saving the resulting stable, low-potential energy structure in the .mol2 file format, ensuring the conformation aligns with physiological conditions[14].

Molecular docking and validation

Docking validation was performed initially to ensure the reliability of the docking protocol. This involved redocking the native ligand into its receptor and calculating the Root Mean Square Deviation (RMSD) using YASARA software (Analyze > RMSD > Molecule). The docking method was considered valid only if the calculated RMSD value was less than 2 Å[15]. Ligand-target protein docking was performed using the PLANTS program under the Windows operating system, utilizing the prepared .mol2 files. The binding site was defined using the command **plants -mode bind ref_ligand .mol2 5 protein.mol2**, followed by the docking screen command **plants –mode screen pc_4pyp.txt**[16].

Visualization and drug-likeness analysis

The docking results were ranked based on the binding affinity, with the lowest (most negative) score indicating the most stable interaction. The resulting ligand-protein complexes and their molecular interactions were visualized using Discovery

Studio Visualizer[14]. Drug-likeness was assessed via the Drug Scan based on Lipinski's Ro5. Parameters evaluated included a Molecular Weight (MW) of <500 g/mol, lipophilicity (LogP) of <5, hydrogen bond donor (HBD) count of <5, hydrogen bond acceptor (HBA) count of <10, and a molar refractivity (MR) between 40-130.

Data analysis

The pharmacokinetic activity and toxicity profiles of the test ligands were predicted by uploading their structures to the pkCSM website[17]. This platform allowed for the prediction of various ADMET (absorption, distribution, metabolism, excretion, and toxicity) properties essential for drug development. To validate the stability of the protein-ligand complexes, molecular dynamics (MD) simulations were performed using a program supported by Google Colab and hosted on GitHub. This simulation utilized the OpenMM engine and the AMBER force field (specifically FF19SB for protein and GAFF2 for the ligand, with TIP3P water type). The setup involved installing necessary Python libraries and packages (including Anaconda, PyTraj, Py3Dmol, ProLIF, NumPy, Matplotlib, and AmberTools) via Google Colab, followed by connecting to Google Drive for data storage. Simulation parameters were set to minimize the system over 1000 steps, and the equilibration phase was run with appropriate temperature and pressure settings for a simulation time of 100 ns. The stability of the complex was analyzed by monitoring the fluctuations in potential energy, RMSD, and RMSF (Root Mean Square Fluctuation)[18]. Stable fluctuations were key to confirming the reliability of the docking results.

RESULTS AND DISCUSSION

Receptor analysis for this study focused on estrogen-type receptors, with the specific PDB codes selected being 2QA8, 1X7R, 1X7J, 1QKM, and 6QGG. These receptor structures were downloaded in PDB file format from the official PDB website. The resolution and native ligands associated with each receptor are detailed in **Table I**. A lower receptor resolution value is a critical factor in molecular docking, as resolutions below 3 Å are generally preferred. A lower resolution signifies a higher quality crystallographic structure, which directly correlates with improved receptor stability and more accurate ligand pose prediction during the computational docking process[19].

Table I. Receptor used.

PDB ID	Experimental method	Molecules	Native ligand	Resolution (Å)
1QKM	X-ray difraction	ER-β	Genistein	1.80
1X7J	X-ray difraction	ER-β	Genistein	2.30
1X7R	X-ray difraction	ER-α	Genistein	2.00
2QA8	X-ray difraction	ER-α	Genistein	1.85
6QGG	X-ray difraction	Bcl-2	[(3~{R})-3-[[4-[[4-[4-[[2-(4-chlorophenyl)phenyl]methyl]piperazin-1-yl]phenyl]carbonylsulfamoyl]-2-nitro-phenyl]amino]-4-phenylsulfanyl-butyl]-(2-hydroxy-2-oxoethyl)-dimethyl-azanium	1.50

Target receptor analysis was performed to determine the quality and structural stability of the selected proteins by evaluating their Ramachandran plot profiles via the PDBSum web server. This critical parameter confirms the stereochemical correctness of the protein backbone[20]. As detailed in **Table II**, all five selected protein structures demonstrated excellent quality and stability. Specifically, PDB codes 1QKM (96.6%), 1X7J (93.7%), 1X7R (95.5%), 2AQ8 (94.3%), and 6QGG (96.0%) all showed a high percentage of amino acid residues located in the most favored regions and a universally low 0.0% presence in the disallowed regions. These results confirm that all five receptor structures are reliable and structurally stable for use in subsequent molecular docking studies. The five receptor structures were strategically selected based on their relevance to the estrogen signaling pathways, their high-resolution quality (≥3 Å), and their representation of different receptor subtypes (ER-α, ER-β, and specific apoptosis-related receptors)[21]. This selection strategy ensures a comprehensive assessment of ligand compatibility across functionally and conformationally distinct receptor targets.

Table II. Ramachandran plot analysis.

PDB ID	Residues in most favored regions (%)	Residues in additionally allowed regions (%)	Residues in disallowed regions (%)	Overall model quality assessment
1QKM	96.6	3.4	0.0	Very high quality & Stable
1X7J	93.7	6.3	0.0	High quality & Stable
1X7R	95.5	4.5	0.0	Very high quality & Stable
2QA8	94.3	5.7	0.0	High quality & Stable
6QGG	96.0	4.0	0.0	Very high quality & Stable

The initial validation of the receptor structures, critical for accurate molecular docking, is presented in **Table III**. Out of the five protein structures assessed, only two (1QKM (RMSD: 1.1306 Å; Binding affinity: -94.5783 kcal/mol) and 1X7R (RMSD: 1.1549 Å; Binding affinity: -90.2397 kcal/mol) fulfilled the stringent docking validation criteria by exhibiting an RMSD value below 2.0 Å. This low RMSD confirms the reliability and predictive accuracy of the docking protocol for these specific structures[22]. Consequently, 1QKM and 1X7R were selected for all subsequent detailed docking and simulation analyses[23]. The remaining structures (1X7J, 2QA8, and 6QGG), which yielded significantly higher RMSD values (7.1085 Å, 7.0271 Å, and 14.0229 Å, respectively), were excluded from the primary investigation, although their data are included in the table for transparency.

Table III. Docking method validation results.

PDB ID	Binding affinity (kcal/mol)	RMSD (Å)	Validation Status
1QKM	-94.58	1.13	Successful
1X7J	-90.24	1.15	Successful
1X7R	-85.25	7.11	Failed
2QA8	-89.58	7.03	Failed
6QGG	+60.60	14.02	Failed

The subsequent molecular docking of the test ligands with the selected target receptors was executed using the PLANTS program via the command-line interface (CMD). The active site for each receptor was precisely defined by referencing the coordinates of the native ligand's position. A grid box, measuring 20 x 20 x 20 Å, was centered over this ligand-binding site to encompass the relevant cavity fully. The test set comprised 23 compounds derived from *M. oleifera* leaf secondary metabolites, alongside established comparative drugs. Analysis focused on the three *M. oleifera* compounds that exhibited the lowest (most negative) binding affinity values across the receptors, as a smaller binding affinity value signifies a stronger, more stable interaction between the ligand and the receptor[22]. These top three compounds were then directly compared against the binding affinities of the native ligands and the comparative drugs. The complete results of the test ligand docking for each validated receptor are detailed in **Table IV**.

Table IV. Analysis of docking results on the 1QKM receptor.

Compounds	Source/category	Binding affinity (kcal/mol)
Reference compounds		
Natural ligand (1QKM)	Reference	-94.58
Cyclophosphamide	Reference drug	-67.59
Ligands from M. oleifera		
Genistein	*Moringa oleifera*	-96.46
Luteolin	*Moringa oleifera*	-91.67
Apigenin	*Moringa oleifera*	-88.45
Niazimicin	*Moringa oleifera*	-86.05
Quercetin	*Moringa oleifera*	-85.72
Kaempferol	*Moringa oleifera*	-84.32
Niazirin	*Moringa oleifera*	-83.77
Myricetin	*Moringa oleifera*	-80.93
Benzylglucosinolate	*Moringa oleifera*	-80.47
2-Metilpropil glukosinolat	*Moringa oleifera*	-79.42
Glucococlearin	*Moringa oleifera*	-79.08
Glucoputranjivin	*Moringa oleifera*	-75.95
Eugenol	*Moringa oleifera*	-68.78
Niazirinin	*Moringa oleifera*	-67.38
Benzyl isothiocyanate	*Moringa oleifera*	-62.70
Moringine	*Moringa oleifera*	-61.62
Benzylamine	*Moringa oleifera*	-61.64
Epicatechin	*Moringa oleifera*	-60.95

Niaziminin	*Moringa oleifera*	-55.95
Lupeol	*Moringa oleifera*	-45.07
Quercetin-3-O-glucoside	*Moringa oleifera*	-32.61
Rutin	*Moringa oleifera*	80.58
4-O-α-L-Rhamnopyranosylglucosinalbin	*Moringa oleifera*	14.63

The results of the docking analysis against the 1QKM identified three compounds from *M. oleifera* leaves that exhibited binding affinities superior to both the native ligand and the reference drug, cyclophosphamide. Specifically, genistein showed the strongest affinity with a binding energy of -96.4564 kcal/mol, followed by Luteolin at -91.67 kcal/mol, and apigenin at -88.4475 kcal/mol. Cyclophosphamide, chosen as the comparator drug due to its frequent clinical use in breast cancer therapy and its well-characterized binding profile with ERs, serves as a crucial benchmark for assessing the therapeutic potential of the natural compounds in this study[24]. The significantly more negative binding energy values demonstrated by genistein, luteolin, and apigenin suggest that these compounds may possess a higher affinity and more stable interaction with the 1QKM receptor than the standard chemotherapeutic agent.

Molecular docking simulations against the 1X7J receptor (**Table V**) revealed three key compounds from *M. oleifera* leaf extract that exhibited superior binding affinities compared to both the native ligand and the reference drug, cyclophosphamide. Specifically, the top-performing compounds were apigenin, with a binding affinity of -87.6074 kcal/mol; genistein, showing an affinity of -90.8068 kcal/mol; and luteolin, which demonstrated the strongest interaction with an affinity of -92.238 kcal/mol. These findings indicate that apigenin, genistein, and luteolin, among all tested secondary metabolites, possess the most favorable predicted interactions and strongest docking scores toward the target receptor, suggesting their potential as promising candidates for further pharmacological investigation.

Table V. Analysis of docking results on the 1X7J receptor.

Compounds	Source/category	Binding affinity (kcal/mol)
Reference compounds		
Natural ligand (1X7J)	Reference	-90.24
Cyclophosphamide	Reference drug	-66.39
Ligands from M. oleifera		
Quercetin	*Moringa oleifera*	-84.54
Kaempferol	*Moringa oleifera*	-82.99
Myricetin	*Moringa oleifera*	-81.69
Genistein	*Moringa oleifera*	-90.81
Eugenol	*Moringa oleifera*	-63.59
Benzyl isothiocyanate	*Moringa oleifera*	-60.16
Benzylamine	*Moringa oleifera*	-61.60
Luteolin	*Moringa oleifera*	-92.24
Epicatechin	*Moringa oleifera*	-73.16
Glucococlearin	*Moringa oleifera*	-87.06
Glucoputranjivin	*Moringa oleifera*	-81.97
Lupeol	*Moringa oleifera*	-46.38
Moringine	*Moringa oleifera*	-61.59
Niazimicin	*Moringa oleifera*	-83.27
Quercetin-3-O-glucosides	*Moringa oleifera*	-55.36
Rutin	*Moringa oleifera*	33.08
Apigenins	*Moringa oleifera*	-87.61
Niazirine	*Moringa oleifera*	-81.91
Niaziminin	*Moringa oleifera*	-68.83
Niazirinine	*Moringa oleifera*	-70.38
2-Methylpropyl glucosinolate	*Moringa oleifera*	-84.63
4-O-α-L-Rhamnopyranosylglucosinalbin	*Moringa oleifera*	-30.38
Benzylglucosinolate	*Moringa oleifera*	-81.31

The assessment of molecular interactions between the ligand and the target protein was performed through visualization using Discovery Studio software. The primary objective of this visualization was to elucidate the specific interactions, notably hydrogen bonds and hydrophobic bonds, that stabilize the ligand-protein complex, thereby predicting binding affinity and mechanism. Hydrogen bonds, critical for drug properties and stability, represent a strong type of dipole-dipole interaction. They form when a partially positive hydrogen atom, bonded to a highly electronegative atom (like O, N, or F), is attracted to the lone pair of electrons on another electronegative atom[25]. Concurrently, hydrophobic bonds—interactions among nonpolar molecules that cluster away from the aqueous environment—also significantly contribute to complex

stability, often forming within the globular interior of the protein[26]. Furthermore, crucial to evaluating the compound's potential as a therapeutic agent are its pharmacokinetic parameters, which are summarized in **Table VI**. These include the logP value, typically predicted using tools such as SwissADME or pkCSM. The logP value serves as a fundamental metric for assessing the lipophilicity and subsequent absorption potential of the compounds under investigation.

Table VI. Comparison of hydrogen and hydrophobic bonds.

Receptors	Compound	Hydrogen bonds	Hydrophobic bonds
1QKM	Natural ligands	ARG346, HIS475, LEU339	MET295, LEU426, THR299, MET336, LEU298, LEU301, GLU305, LEU343, PHE356, MET340, ALA302, LEU380, ILE326, ILE373, GLY472, MET479
	Apigenin	ARG34, LEU339	GLY472, ILE376, LEU298, LEU380, MET340, LEU340, PHE356, LEU301, ALA302, MET336, VAL487, THR299, LEU476, MET295, HIS475, ILE373
	Genistein	LEU339, ARG346, HIS475	LEU343, PHE356, LEU380, MET340, ALA302, ILE376, GLY472, ILE373, MET479, MET295, LEU476, THR299, MET336, LEU298, LEU301, GLU305
	Luteolin	ARG346, GLU305	PHE356, LEU339, LEU343, LEU380, PHE377, ILE326, LEU476, GLY472, ILE373, HIS475, MET299, THR299, LEU298, MET336, MET340, LEU301, ALA302
1X7J	Natural ligands	ARG346, LEU339, HIS425	MET340, LEU380, ILE376, GLY422, ILE373, MET295, THR299, LEU298, MET336, ALA302, LEU301, LEU343, PHE356
	Apigenin	ARG346, LEU339	GLU305, LEU301, MET336, THR299, LEU476, MET295, HIS475, ILE373, GLY422, ILE376, LEU298, ALA302, LEU380, PHE356, MET340, LEU343
	Genistein	HIS475, ARG346, LEU339	MET479, LEU476, MET295, THR299, LEU298, MET336, ALA302, LEU301, LEU343, PHE356, GLU305, MET340, LEU380, ILE376, GLY422, ILE373
	Luteolin	ARG346, GLU305, GLY472	PHE356, LEU343, LEU339, MET340, LEU380, ILE376, ILE373, HIS475, MET295, MET479, THR299, LEU298, LEU476, MET336, ALA302, LEU301

Analysis of the molecular docking simulations was crucial for predicting the interaction profiles between the natural compounds (apigenin, genistein, and luteolin) and the target proteins. Specifically, the binding of the native ligand to the 1QKM receptor was modeled computationally to establish a reference for stable ligand-protein complex formation. Visualization of these results indicated that the binding characteristics of apigenin closely mirrored those of the native ligand. Apigenin shared the hydrogen-bonding residues Arg346 and Leu339, along with a substantial overlap in hydrophobic interactions involving residues such as Met295, Leu476, Thr299, Met336, Leu298, Leu301, Leu343, Phe356, Met340, Ala302, Leu380, Ile376, Ile373, and Gly479. Intriguingly, the binding pattern of genistein demonstrated an identical profile of both hydrogen and hydrophobic bonds to that of the native ligand. For luteolin, the shared hydrogen-bonding residue was Arg346, and the overlapping hydrophobic resienables Leu343, Leu380, Ile376, Leu476, Gly472, Ile373, Thr299, Leu298, Met336, Met340, Leu301, and Ala302. The establishment of hydrogen bonds is critical as it imparts stability and high potential binding energy to the protein-ligand complex, while the prevalence of hydrophobic interactions is a fundamental characteristic of the stable structural complex component in receptor binding algorithms.

Further investigation using the 1X7J receptor revealed similar competitive binding behavior. The apigenin compound exhibited shared hydrogen bonding with the native ligand at residues Arg346 and Leu339. The hydrophobic interactions for apigenin involved the common residues Glu305, Leu301, Met336, Thr299, Leu476, Met295, Ile373, Gly422, Ile376, Leu298, Ala302, Leu380, Phe356, Met340, and Leu343. Consistent with the 1QKM results, the genistein compound again displayed an identical set of hydrogen and hydrophobic binding characteristics to the native ligand at the 1X7J site. Finally, luteolin formed a shared hydrogen bond at Arg346, with overlapping hydrophobic interactions involving Phe356, Leu343, Met340, Leu380, Ile376, Ile373, Met295, Met479, Thr299, Leu298, Leu476, Met336, Ala302, and Leu301. The significant structural complementarity demonstrated by these natural ligands, particularly the consistent replication of key binding residues, suggests a high potential for inhibitory activity via a mechanism comparable to that of the native ligand.

The drug-likeness of the candidate compounds was assessed using a Drug Scan analysis, which specifically evaluated compliance with the Ro5 parameters. The Ro5 serves as a critical filter in early-stage drug discovery, predicting the oral bioavailability and passive membrane permeability of potential drug candidates. A compound is considered likely to exhibit good absorption and permeability if it adheres to the following criteria: MW $\leq$500 Daltons, LogP $\leq$5, HBD $\leq$5, and HBA $\leq$10. An additional, though less stringent, parameter often considered is that the Molar Refractivity (MR) must fall within the range of 40 to 130[27]. The MW criterion is crucial, as molecules exceeding 500 Daltons typically encounter difficulty in passively diffusing across the cell membrane, which can significantly impair drug distribution and overall efficacy. Analysis of the three top-performing compound candidates, as detailed in **Table VII**, confirmed that all compounds successfully

satisfied every parameter of the Lipinski Ro5, suggesting a favorable profile for oral bioavailability and establishing their potential as promising drug leads.

Table VII. ADMET properties of compounds based on Ro5.

Compounds	Absorption: Solubility (Log mol/L)	Distribution: VD_{SS} (Log L/kg)	Metabolism: CYP Substrate	Excretion: OCT2 Substrate	Toxicity: Maximum Tolerated Dose (Log mg/kg/day)
Apigenin	-3.329	0.822	CYP2D6: No CYP3A4: No	No	-0.328
Genistein	-3.595	0.094	CYP2D6: No CYP3A4: No	No	0.478
Luteolin	-3.094	1.153	CYP2D6: No CYP3A4: No	No	0.499

Predictive pharmacokinetic and toxicity profiling, collectively known as ADMET, is critical for assessing the *in vivo* fate and potential safety of drug candidates in humans. Favorable pharmacokinetic parameters, particularly robust absorption and wide distribution, correlate directly with increased bioavailability and a higher likelihood of effective receptor interaction[28]. In this study, the ADMET properties for apigenin, genistein, and luteolin were computationally predicted using the pkCSM web platform. While pkCSM offers a broad range of outputs, the analysis prioritized parameters highly relevant to oral drug development, including water solubility (logS), steady-state volume of distribution (log VD_{SS}), and key toxicity endpoints such as hepatotoxicity and Ames toxicity. The detailed results are presented in **Table VIII**.

Absorption potential was evaluated based on logS. Low water solubility (logS <-6) generally impedes enteral absorption[17]. All three compounds exhibited favorable, high water solubility: apigenin (logS: -3.329 log mol/L), genistein (logS: -3.595 log mol/L), and luteolin (logS: -3.094 log mol/L). This suggests good potential for oral bioavailability.

The log VD_{SS} parameter, expressed as log L/kg, provides insight into the drug's distribution tendency between plasma and tissues. A high VDSS indicates extensive tissue distribution, whereas a low value suggests confinement primarily to the plasma compartment. A low distribution is defined as log VD_{SS} <-0.15 log L/kg, and a high distribution is log VD_{SS} >0.45 log L/kg[17]. Apigenin and genistein demonstrated low predicted log VD_{SS} values, suggesting limited tissue partitioning, while Luteolin, with a value of 1.153 log L/kg, showed moderate tissue distribution, placing it within the acceptable range.

Assessment of metabolism focused on the compounds' likelihood of being substrates for the Cytochrome P450 (CYP) isoforms CYP2D6 and CYP3A4, as inhibition or induction of these enzymes can significantly alter the pharmacokinetics of co-administered drugs[29]. Remarkably, the computational prediction indicated that all three compounds were not metabolized by the P450 enzymes, suggesting a low potential for drug-drug interactions mediated by these major metabolic pathways.

For excretion, the compounds were screened for substrate potential towards the renal transporter Organic Cation Transporter 2 (OCT2), which is critical for drug clearance[17]. The prediction showed that apigenin, genistein, and luteolin were not substrates for OCT2. This negative result is favorable, indicating a low risk of adverse drug-drug interactions when co-administered with OCT2 inhibitors, which would otherwise complicate renal clearance and potentially lead to toxicity.

Toxicity prediction encompassed Ames toxicity and hepatotoxicity, with all three compounds showing favorable results for non-mutagenicity (non-Ames toxic) and non-hepatotoxicity. The Maximum Tolerated Dose (MTD), which estimates the recommended initial dose threshold in Phase I clinical trials, was also evaluated. A low MTD is considered <0.477 log(mg/kg/day)[17]. Apigenin yielded a low MTD of 0.328 log(mg/kg/day), while genistein and luteolin had slightly higher, yet still moderate, values of 0.478 log(mg/kg/day) and 0.499 log(mg/kg/day), respectively.

Overall, apigenin exhibited the most promising ADMET profile, demonstrating high water solubility and an acceptable distribution, followed closely by genistein and luteolin. The collective absence of predicted hepatotoxicity, Ames toxicity, CYP450 metabolism, and OCT2 substrate activity suggests that these ligands are compelling oral drug candidates for anticancer development. The computational identification of genistein, luteolin, and apigenin as promising anti-breast cancer lead molecules has important practical implications. These compounds can serve as scaffolds for synthetic modification to further optimize their pharmacokinetic properties and target affinity. Furthermore, standardized extracts rich in these compounds could be explored as dietary supplements for chemoprevention or as adjuvant therapy alongside conventional chemotherapy. The favorable safety and pharmacokinetic profiles support the progression to targeted *in vitro*

cytotoxicity assays and *in vivo* animal studies to fully validate their anticancer efficacy and potential to minimize the side effects of toxic chemotherapeutic agents.

Table VIII. Predictive analysis of ADMET pharmacokinetics with pkCSM.

Compounds	Molecular weight (g/mol)	H-bond donors	H-bond acceptors	LogP	Molar refractivity (MR)	Passes Ro5?
Apigenin	270.24	3	5	2.419	70.813	Yes
Genistein	286.24	4	6	2.125	72.478	Yes
Luteolin	270.24	3	5	2.419	70.813	Yes

Molecular dynamics simulations were executed to assess the stability and conformational behavior of complexes involving two target receptors, their respective native ligands, the comparator drug cyclophosphamide, and the most promising test compounds: apigenin, genistein, and luteolin. These simulations, conducted for a duration of 100 ns, were designed to mimic near-physiological conditions to provide insight into the dynamic interactions within the protein-ligand system over time. The computational environment used for running the MD simulations was Google Colaboratory, a cloud-based service that leverages Jupyter Notebooks linked to Google Drive accounts, facilitating interactive data processing and analysis, particularly for demanding computational tasks[18]. For example, the Ambertools Suite[22] was employed for the simulation setup and analysis. Key metrics obtained from the Ambertools output include the visualization of ligand interactions, the RMSD, and the RMSF. The RMSD values are critical indicators used to evaluate the overall conformational stability of the protein-ligand complexes throughout the 100 ns trajectory. A stable RMSD trend suggests that the protein structure remains stable during the simulation. Concurrently, the RMSF provides a measure of the flexibility of the amino acid residues that constitute the receptor, offering insight into which regions exhibit the most significant mobility upon ligand binding[16].

Molecular dynamics simulations were performed to assess the stability and dynamic behavior of the protein-ligand complexes for the tested compounds (genistein, apigenin, and luteolin) compared to the native ligand and cyclophosphamide within the active sites of both 1QKM and 1X7J receptors. This analysis was primarily based on the RMSD and RMSF trajectories. The RMSD plots for the 1QKM receptor complexes (**Figures 1** to **3**) generally demonstrated an initial phase of structural stability, with the system stabilizing around 1.5 ± 0.25 Å for the majority of the simulation time. This stable baseline indicates that all complexes have attained a maximally stable conformation, thereby maintaining the structural integrity of both the enzyme and the bound ligand.

However, complex-specific deviations were observed. The genistein complex (**Figure 1**) exhibited an observable increase in RMSD to approximately 2.5 Å after the 30-ns mark, signifying a moderate conformational change, possibly representing an "opening" or significant shift in the protein structure. This structural rearrangement may correspond to the ligand exploring alternative, more optimal binding coordinates within the newly accessible pocket. For both the apigenin (**Figure 2**) and luteolin (**Figure 3**) complexes, a similar deviation to approximately 2.0 Å occurred around the 50-ns mark. These transient fluctuations are typically indicative of the protein undergoing a localized conformational "breathing" motion, where the ligand actively searches or reorients to its most favorable binding position. The subsequent return to a stable RMSD, particularly evident in the luteolin complex, affirms that the overall protein-ligand interaction remained stable and favorable following the dynamic adjustment.

Similarly, the MD trajectories for the 1X7J receptor complexes (**Figures 4** to **6**) initially maintained a stable RMSD around 1.5 Å. This consistent stability across complexes underscores the preservation of the native protein conformation and the persistence of favorable ligand-residue interactions. A significant conformational change was observed for the luteolin and genistein complexes (**Figures 4** and **5**), where the RMSD sharply increased to approximately 2.5 Å around the 50-ns and 30-ns marks, respectively. This spike suggests a significant structural rearrangement in the enzyme's backbone, potentially allowing the ligand to attain a more energetically stable, final binding coordination. The apigenin complex (**Figure 6**) displayed a more pronounced spike to 3.0 Å around 50 ns, followed by an additional, minor transient adjustment near 70 ns. Despite these fluctuations, the rapid restabilization confirms the robustness and ultimate integrity of the protein-ligand interactions, suggesting that the tested compounds successfully achieved sustained, stable binding poses within the active site.

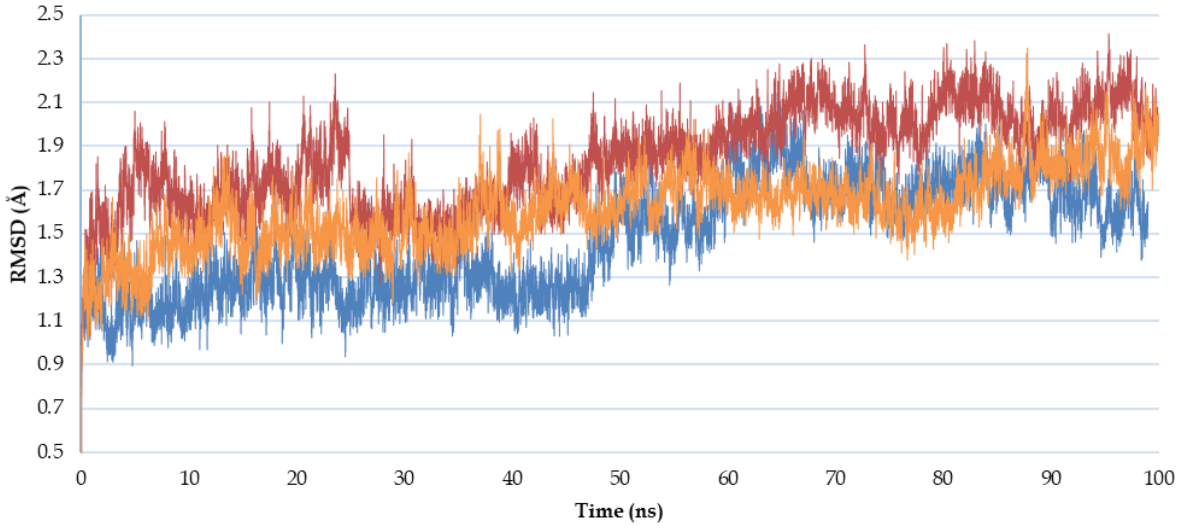

Figure 1. RMSD of MD at 1QKM receptor. Blue: genistein; Red: native ligand; Yellow: cyclophosphamide.

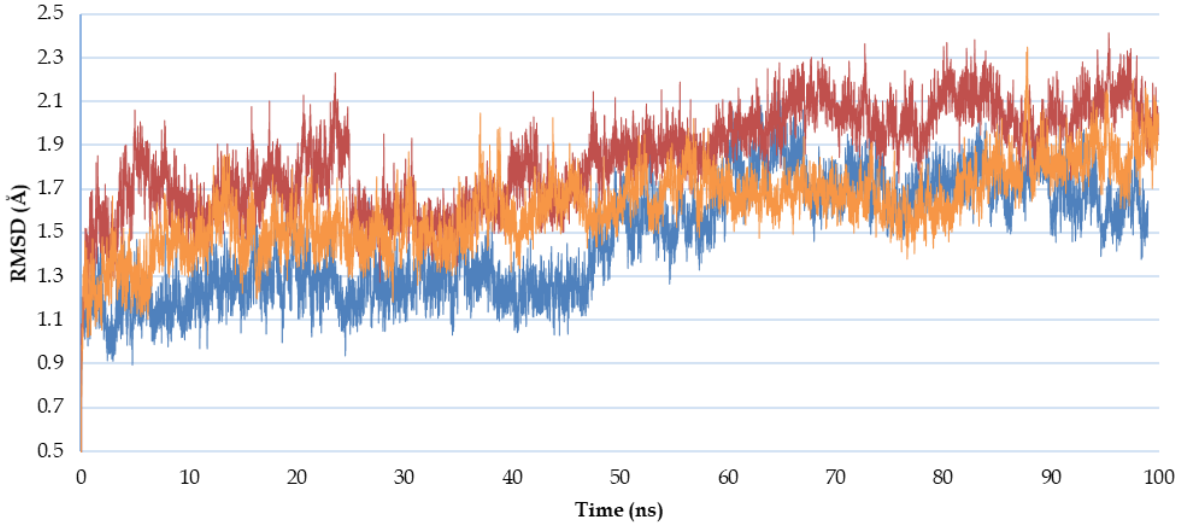

Figure 2. RMSD of MD at 1QKM receptor. Blue: apigenin; Red: native ligand; Yellow: cyclophosphamide.

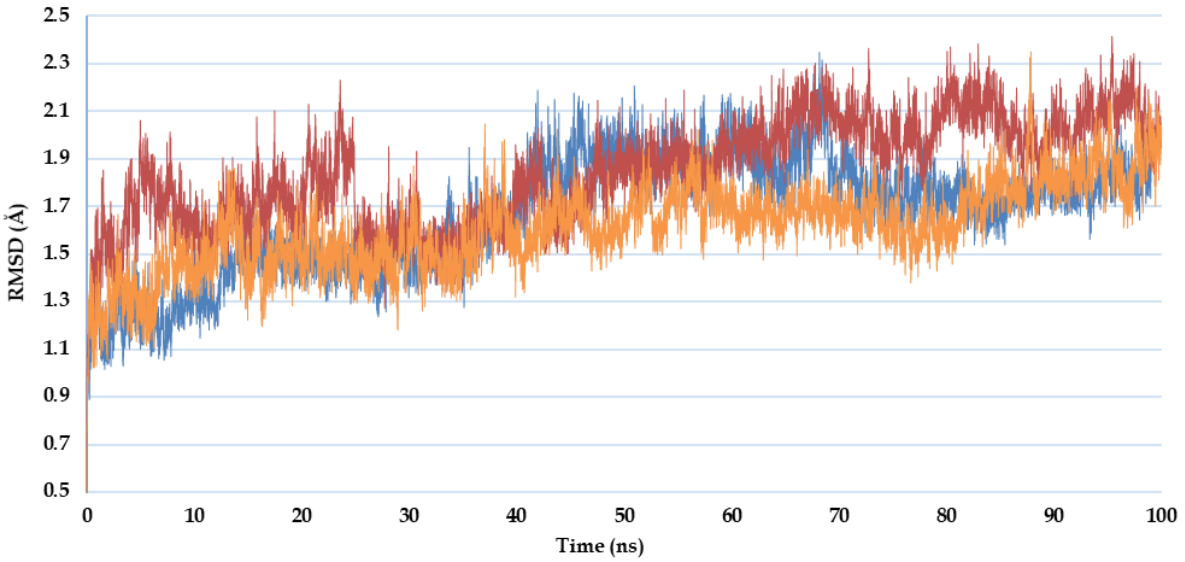

Figure 3. RMSD of MD at 1QKM receptor. Blue: luteolin; Red: native ligand; Yellow: cyclophosphamide.

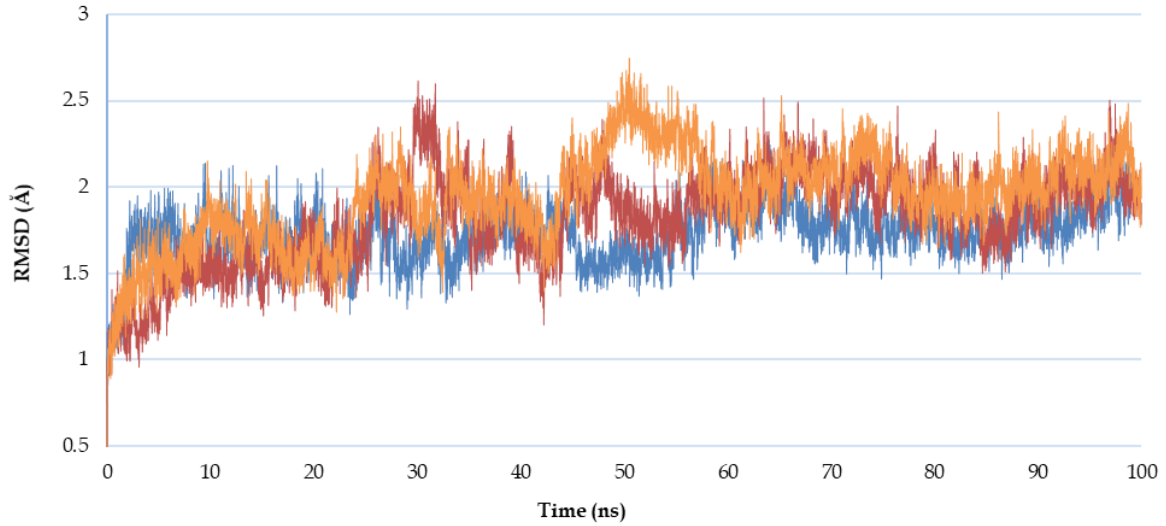

Figure 4. RMSD of MD at 1X7J receptor. Blue: luteolin; Red: native ligand; Yellow: cyclophosphamide.

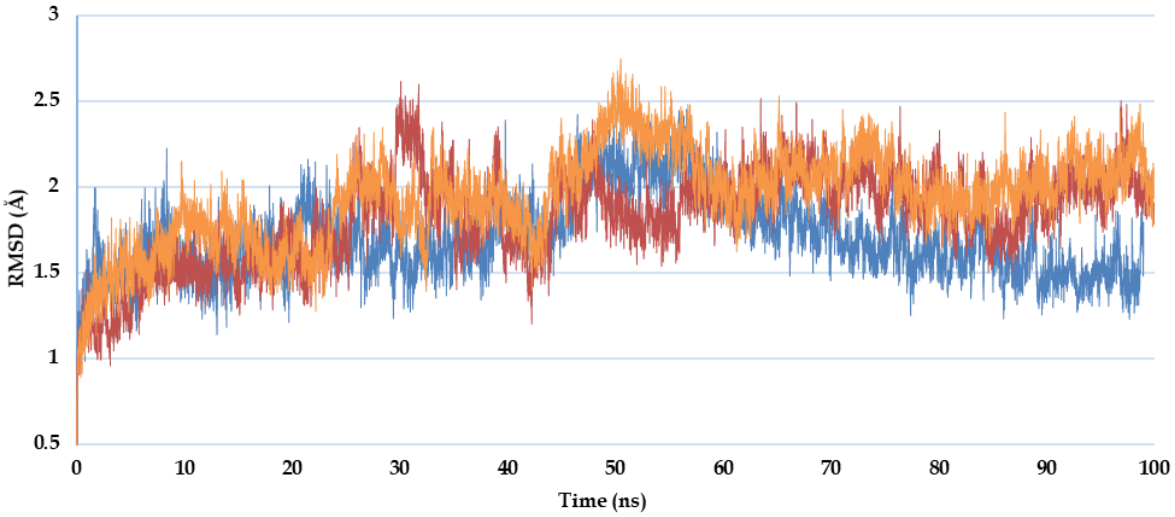

Figure 5. RMSD of MD at 1X7J receptor. Blue: genistein; Red: native ligand; Yellow: cyclophosphamide.

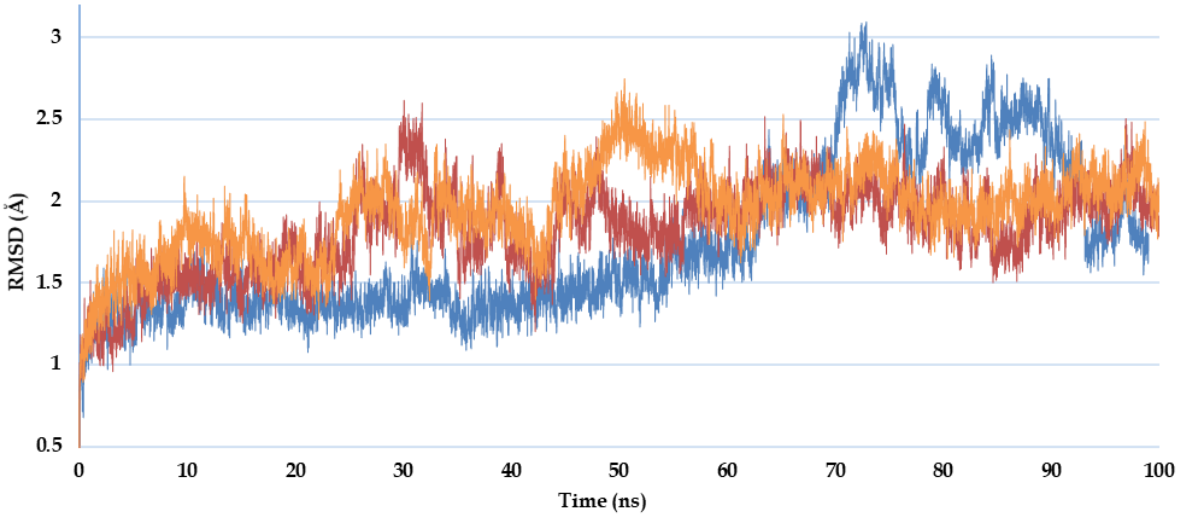

Figure 6. RMSD of MD at 1X7J receptor. Blue: apigenin; Red: native ligand; Yellow: cyclophosphamide.

The RMSF analysis provides critical insight into the localized dynamic flexibility of the receptor backbone upon ligand binding (**Figures 7** to **12**). For both the 1QKM and 1X7J receptors, all three compounds (genistein, apigenin, and luteolin) consistently exhibited remarkably stable interactions. The RMSF values for the majority of the amino acid residues across both receptors remained confined within the narrow range of 0 to 1.5 Å (typically 0 to 1.0 Å for the most rigid parts) throughout the simulation.

This low and uniform RMSF profile is a powerful indicator of a rigid and stable binding pocket, implying that the binding events do not induce significant conformational changes or excessive localized flexibility in the receptor backbone. Since the magnitude of RMSF is directly proportional to a residue's flexibility, these results strongly suggest that the established interaction between the ligands and their corresponding amino acid residues is well-sustained, minimally disruptive, and indicative of a high-affinity, sustained binding mode. The minimal fluctuations confirm the stability observed in the RMSD plots and underscore the effective binding of the tested compounds[30].

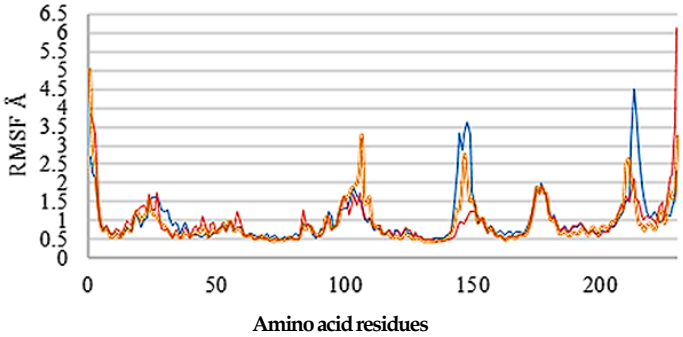

Figure 7. RMSF of MD at 1QKM receptor. Blue: genistein; Red: native ligand; Yellow: cyclophosphamide.

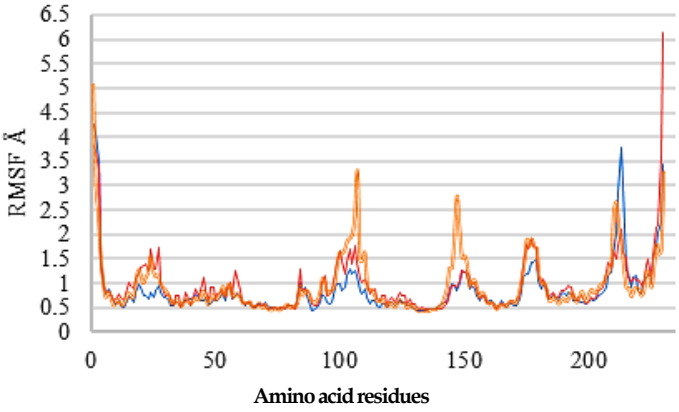

Figure 8. RMSF of MD at 1QKM receptor. Blue: apigenin; Red: native ligand; Yellow: cyclophosphamide.

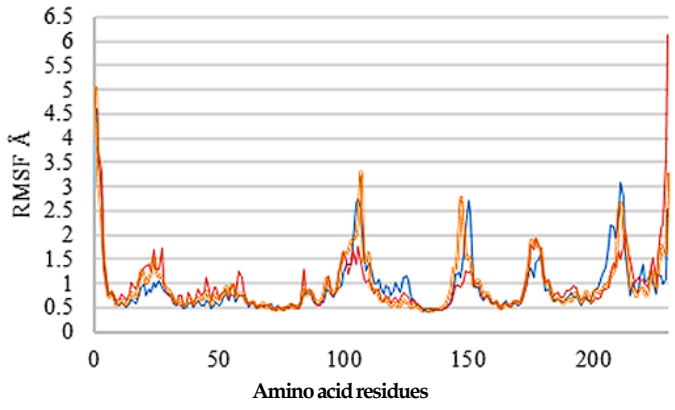

Figure 9. RMSF of MD at 1QKM receptor. Blue: luteolin; Red: native ligand; Yellow: cyclophosphamide.

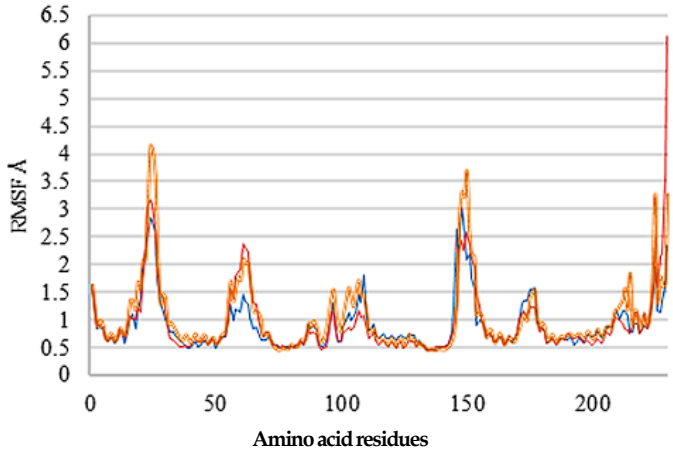

Figure 10. RMSF of MD at 1X7J receptor. Blue: luteolin; Red: native ligand; Yellow: cyclophosphamide.

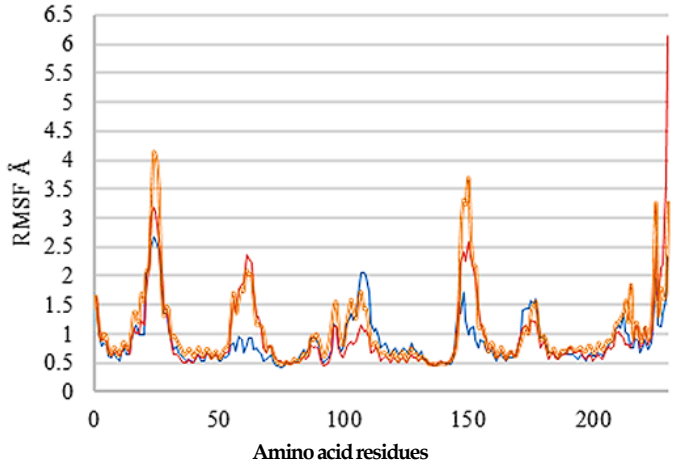

Figure 11. RMSF of MD at 1X7J receptor. Blue: genistein; Red: native ligand; Yellow: cyclophosphamide.

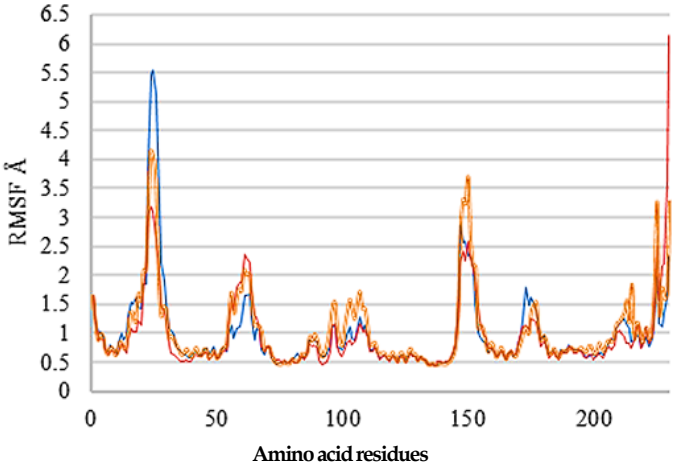

Figure 12. RMSF of MD at 1X7J receptor. Blue: apigenin; Red: native ligand; Yellow: cyclophosphamide.

CONCLUSION

Based on the comprehensive computational analysis, three key metabolites derived from *M. oleifera* demonstrated superior interactions and stability with the ER targets. Specifically, genistein exhibited the most favorable binding affinity (binding energy –96.4564 kcal/mol) toward the 1QKM target, followed closely by luteolin (–92.238 kcal/mol at 1X7J) and apigenin (–88.4475 kcal/mol at 1QKM). Furthermore, all three lead compounds maintained stable RMSD profiles throughout the

100-ns MD simulations, confirming the robustness and longevity of their predicted binding modes to the ERs. Crucially, the subsequent pharmacokinetic and toxicity assessments indicated favorable absorption and distribution characteristics alongside no predicted hepatotoxicity. Collectively, these findings strongly endorse genistein, luteolin, and apigenin as promising, orally bioavailable candidates for further development as novel anticancer agents targeting ERs.

ACKNOWLEDGMENT

The authors gratefully acknowledge the invaluable support provided by Universitas Bakti Tunas Husada, without which this research endeavor would not have been possible.

AUTHORS' CONTRIBUTION

Conceptualization: Saeful Amin, Vanessa Angelica Sheryl
Data curation: Saeful Amin
Formal analysis: Saeful Amin, Vanessa Angelica Sheryl, Ade Yeni Aprillia, Anisa Pebiansyah
Funding acquisition: Saeful Amin
Investigation: Vanessa Angelica Sheryl
Methodology: Saeful Amin
Project administration: Saeful Amin, Anisa Pebiansyah
Resources: Saeful Amin
Software: Saeful Amin
Supervision: Saeful Amin, Ade Yeni Aprillia, Anisa Pebiansyah
Validation: Saeful Amin
Visualization: Saeful Amin
Writing - original draft: Saeful Amin, Vanessa Angelica Sheryl
Writing - review & editing: Saeful Amin, Ade Yeni Aprillia, Anisa Pebiansyah

DATA AVAILABILITY

None.

CONFLICT OF INTEREST

The authors declared no conflict of interest related to this research.

REFERENCES

1. Łukasiewicz S, Czeczelewski M, Forma A, Baj J, Sitarz R, Stanisławek A. Breast Cancer-Epidemiology, Risk Factors, Classification, Prognostic Markers, and Current Treatment Strategies-An Updated Review. Cancers. 2021;13(17):4287. DOI: 10.3390/cancers13174287; PMCID: PMC8428369; PMID; 34503097

2. Zhang YN, Xia KR, Li CY, Wei BL, Zhang B. Review of Breast Cancer Pathologigcal Image Processing. Biomed Res Int. 2021;2021:1994764. DOI: 10.1155/2021/1994764; PMCID: PMC8478535; PMID: 34595234

3. Sultan R, Ahmed A, Wei L, Saeed H, Islam M, Ishaq M. The anticancer potential of chemical constituents of Moringa oleifera targeting CDK-2 inhibition in estrogen receptor positive breast cancer using in-silico and in vitro approaches. BMC Complement Med Ther. 2023;23(1):396. DOI: 10.1186/s12906-023-04198-z; PMCID: PMC10625284; PMID: 37925393

4. Wang J, Wu SG. Breast Cancer: An Overview of Current Therapeutic Strategies, Challenge, and Perspectives. Breast Cancer. 2023;15:721-30. DOI: 10.2147/bctt.s432526; PMCID: PMC10596062; PMID: 37881514

5. Habara M, Shimada M. Estrogen receptor α revised: Expression, structure, function, and stability. Bioessays. 2022;44(12):e2200148. DOI: 10.1002/bies.202200148; PMID: 36192154

6. Liu Y, Ma H, Yao J. ERα, A Key Target for Cancer Therapy: A Review. Onco Targets Ther. 2020;13:2183-91. DOI: 10.2147/ott.s236532; PMCID: PMC7073439; PMID: 32210584

7. Atanasov AG, Zotchev SB, Dirsch VM, International Natural Product Sciences Taskforce, Supuran CT. Natural products in drug discovery: advances and opportunities. Nat Rev Drug Discov. 2021;20(3):200-16. DOI: 10.1038/s41573-020-00114-z; PMCID: PMC7841765; PMID: 33510482

8. Kumar S, Murti Y, Arora S, Akram W, Bhardwaj H, Gupta K, et al. Exploring the therapeutic potential of Moringa oleifera Lam. in Traditional Chinese Medicine: A comprehensive review. Pharmacol Res Mod Chin Med. 2024;12:100473. DOI: 10.1016/j.prmcm.2024.100473

9. Amin MF, Ariwibowo T, Putri SA, Kurnia D. Moringa oleifera: A Review of the Pharmacology, Chemical Constituents, and Application for Dental Health. Pharmaceuticals. 2024;17(1):142. DOI: 10.3390/ph17010142; PMCID: PMC10819732; PMID: 38276015

10. Pareek A, Pant M, Gupta MM, Kashania P, Ratan Y, Jain V, et al. Moringa oleifera: An Updated Comprehensive Review of Its Pharmacological Activities, Ethnomedicinal, Phytopharmaceutical Formulation, Clinical, Phytochemical, and Toxicological Aspects. Int J Mol Sci. 2023;24(3):2098. DOI: 10.3390/ijms24032098; PMCID; PMC9916933; PMID: 36768420

11. Soto JA, Gómez AC, Vásquez M, Barreto AN, Molina KS, Zuniga-Gonzalez CA. Biological properties of Moringa oleifera: A systematic review of the last decade. F1000Res. 2025;13:1390. DOI: 10.12688/f1000research.157194.2; PMCID; PMC11782934; PMID: 39895949

12. Tahiroğlu V, Gören K, Bağlan M. In Silico drug evaluation by molecular docking, ADME studies and DFT calculations of 2-(6-chloro-2-(4-chlorophenyl)imidazo[1,2-a]pyridin-3-yl)-N, N-dipropylacetamide. BMC Pharmacol Toxicol. 2025;26(1):116. DOI: 10.1186/s40360-025-00958-4; PMCID: PMC12135494; PMID: 40468388

13. Masarkar N, Ray SK, Saleem Z, Mukherjee S. Potential anti-cancer activity of Moringa oleifera derived bio-active compounds targeting hypoxia-inducible factor-1 alpha in breast cancer. J Complement Integr Med. 2023;21(3):282–94. DOI: 10.1515/jcim-2023-0182; PMID: 37712721

14. Ruswanto R, Nofianti T, Mardianingrum R, Lestari T. Desain dan Studi In Silico Senyawa Turunan Kuwanon-H sebagai Kandidat Obat Anti-HIV. J Kimia Valensi. 2018;4(1):57–66. DOI: 10.15408/jkv.v4i1.6867

15. Pratama MRF, Poerwono H, Siswodihardjo S. Introducing a two‐dimensional graph of docking score difference vs. similarity of ligand‐receptor interactions. Indones J Biotechnol. 2021;26(1):54-60. DOI: 10.22146/ijbiotech.62194

16. Yang C, Chen EA, Zhang Y. Protein-Ligand Docking in the Machine-Learning Era. Moleules. 2022;27(14):4568. DOI: 10.3390/molecules27144568; PMCID: PMC9323102; PMID: 35889440

17. Pires DEV, Blundell TL, Ascher DB. pkCSM: Predicting Small-Molecule Pharmacokinetic and Toxicity Properties Using Graph-Based Signatures. J Med Chem. 2015;58(9):4066-72. DOI: 10.1021/acs.jmedchem.5b00104; PMCID: PMC4434528; PMID: 25860834

18. Trott O, Olson AJ. AutoDock Vina: improving the speed and accuracy of docking with a new scoring function, efficient optimization, and multithreading. J Comput Chem. 2010;31(2):455–61. DOI: 10.1002/jcc.21334; PMCID: PMC3041641; PMID: 19499576

19. Lee S, Kim S, Lee GR, Kwon S, Woo H, Seok C, et al. Evaluating GPCR modeling and docking strategies in the era of deep learning-based protein structure prediction. Comput Struct Biotechnol J. 2022;21:158-67. DOI: 10.1016/j.csbj.2022.11.057; PMCID: PMC9747351; PMID: 36544468

20. Sobolev OV, Afonine PV, Moriarty NW, Hekkelman ML, Joosten RP, Perrakis A, et al. A Global Ramachandran Score Identifies Protein Structures with Unlikely Stereochemistry. Structure. 2020;28(11):1249-58. DOI: 10.1016/j.str.2020.08.005; PMCID: PMC7642142; PMID: 32857966

21. Bafna D, Ban F, Rennie PS, Singh K, Cherkasov A. Computer-Aided Ligand Discovery for Estrogen Receptor Alpha. Int J Mol Sci. 2020;21(12):4193. DOI: 10.3390/ijms21124193; PMCID: PMC7352601; PMID; 32545494

22. Fatima S, Usmani MA, Srivastava AK. Bioactive metabolites of Moringa oleifera with functional activities. Res Pharm. 2024;4:25-37. DOI: 10.25081/rip.2024.v14.9060

23. Terefe EM, Ghosh A. Molecular Docking, Validation, Dynamics Simulations, and Pharmacokinetic Prediction of Phytochemicals Isolated From Croton dichogamus Against the HIV-1 Reverse Transcriptase. Bioinform Bio Insights. 2022;16:11779322221125605. DOI: 10.1177/11779322221125605; PMCID: PMC9516429; PMID: 36185760

24. Tousif M, Nadeem M, Tabassum M, Rizvi MMA, Haque SE. Anticancer efficacy of nerolidol, cyclophosphamide, and their combination against breast cancer cell line MCF-7. Med Oncol. 2024;42(10):430. DOI: 10.1007/s12032-025-02997-7; PMID: 40828487

25. Dogara AM, Al-Sultani ATK, Kadium SMA, Mohammed HA, Al-Taey DKA, Alsaffar MF, et al. Anticancer Potential of moringa oleifera Lam: a Systematic Review. IOP Conf Ser Earth Environ Sci. 2024;1371:052072. DOI: 10.1088/1755-1315/1371/5/052072

26. Dyson HJ, Wright PE, Scheraga HA. The role of hydrophobic interactions in initiation and propagation of protein folding. Proc Natl Acad Sci U S A. 2006;103(35):13057-61. DOI: 10.1073/pnas.0605504103; PMCID: PMC1559752; PMID; 16916929

27. Leeson PD, Bento AP, Gaulton A, Hersey A, Manners EJ, Radoux CJ, et al. Target-Based Evaluation of "Drug-Like" Properties and Ligand Efficiencies. J Med Chem. 2021;64(11):7210-30. DOI: 10.1021/acs.jmedchem.1c00416; PMCID: PMC7610969; PMD: 33983732

28. Sharma V, Paliwal R, Janmeda P, Sharma S. Chemopreventive efficacy of Moringa oleifera pods against 7, 12-dimethylbenz[a]anthracene induced hepatic carcinogenesis in mice. Asian Pac J Cancer Prev. 2012;13(6):2563-9. DOI: 10.7314/apjcp.2012.13.6.2563; PMID: 22938421

29. Deodhar M, Al Rihani SB, Arwood MJ, Darakjian L, Dow P, Turgeon J, et al. Mechanisms of CYP450 Inhibition: Understanding Drug-Drug Interactions Due to Mechanism-Based Inhibition in Clinical Practice. Pharmaceutics. 2020;12(9):846. DOI: 10.3390/pharmaceutics12090846; PMCID: PMC7557591; PMID: 32899642

30. Dewaker V, Park ST, Lee JJ, Kim HS. Discovery and Exploration of Small Molecule Binders for CT83: Computational Insights from Homology Modeling, Virtual Screening, MD Simulations, Interaction Fingerprint, and Network Communications. ACS Omega. 2025;10(22):22884-908. DOI: 10.1021/acsomega.5c00053; PMCID: PMC12163856; PMID: 40521510